

# Surface Plasmon Wave Adapter Designed with Transformation Optics

Jingjing Zhang,\* Sanshui Xiao, Martijn Wubs, and Niels Asger Mortensen\*

DTU Fotonik, Department of Photonics Engineering, Technical University of Denmark, DK-2800 Kongens Lyngby, Denmark

A metal–dielectric interface has the ability of sustaining propagating electromagnetic waves in the form of surface plasmon polaritons (SPPs), which arise from the interaction between free electrons in the metal and electromagnetic radiation. SPP modes in metallic nanostructures allow the control of light at subwavelength scale and give rise to the confinement of electromagnetic fields to the metallic surfaces. SPP propagation<sup>1–7</sup> and scattering<sup>8–11</sup> in metallic nanostructures have been studied experimentally and theoretically, and various shaped nanostructures have been proposed and fabricated to guide SPP modes, including thin metal films,<sup>2,3</sup> cylindrical metal nanorods,<sup>4–6</sup> metal nanostrips, nanogaps in thin metal films,<sup>7</sup> and metal wedge/groove structures.<sup>8</sup> Metal films and strips can guide the SPP modes on a longer range,<sup>2</sup> while metallic wedge/groove structures can achieve subwavelength localization of the guided signals.<sup>8</sup> Surface plasmon polaritons remain nonradiating as long as they propagate on a surface that is translationally invariant in the direction of propagation. Any non-uniformity breaking this symmetry is typically causing severe scattering and coupling to radiation fields. Therefore, broken translational invariance, in the form of surface roughness or other shape non-uniformities, may cause severe scattering of the surface plasmon waves, thereby limiting their applications in the guidance of SPP signals. Here, we propose a wave adapter that enables the confinement of surface plasmon waves on non-uniform metal surfaces and allows for adiabatically coupling of surface plasmon modes between different-sized metallic waveguides connected by a very short taper.<sup>12,13</sup> This wave adapter is designed with the transformation optics (TO),<sup>14,15</sup> a mathematical tool to design artificial media with unusual electromagnetic properties, which has been recently extended to the

**ABSTRACT** On the basis of transformation optics, we propose the design of a surface plasmon wave adapter which confines surface plasmon waves on non-uniform metal surfaces and enables adiabatic mode transformation of surface plasmon polaritons with very short tapers. This adapter can be simply achieved with homogeneous anisotropic naturally occurring materials or subwavelength grating-structured dielectric materials. Full wave simulations based on a finite-element method have been performed to validate our proposal.

**KEYWORDS:** surface plasmon polaritons · transformation optics · metamaterial · nanostructures · wave adapter

area of surface plasmon polaritons,<sup>16–22</sup> in particular, to control the propagation of surface plasmon waves.<sup>20–22</sup> As we discuss in this article, the required dielectric anisotropy of the wave adapter can be realized with naturally occurring birefringent crystals, or subwavelength grating-structured dielectric materials, which give even more flexibility in the design of SPP adapters. Since the adapter is made of materials with small attenuation coefficient, it introduces small loss while reducing the non-adiabatic scattering, thereby enabling an optimum SPP taper which solves the contradiction between adiabaticity and loss in SPP mode transformation between metallic waveguides. The SPP adapter has various prospective applications in the field of nano-optics, where rapid adiabatic mode transformation is required.

## THEORY

On the basis of the principle that certain dielectric media appear to light as if they were changing the geometry of space, one can work in the opposite way to deliberately design materials which can result in the required geometry distortion of space for the light. After applying a proper coordinate transformation to the homogeneous isotropic space, the permittivity and permeability distributions can be derived, so that the light will propagate in desired trajectories. In principle, both the dielectric material and the metal in the plasmonic cases should be

\* Address correspondence to [maggiejzj@gmail.com](mailto:maggiejzj@gmail.com), [asger@mailaps.org](mailto:asger@mailaps.org).

Received for review October 23, 2010 and accepted May 13, 2011.

Published online May 13, 2011  
10.1021/nn200516r

© 2011 American Chemical Society

considered in the TO process in order to control the SPPs. In our studies, we will keep the metal as it is and only apply TO on the dielectric material. This kind of simplified approach has already been adopted in refs 20–22, and here we demonstrate the validity of this simplification in practice by comparing the energies in the dielectric medium and the metal. For a transverse magnetic (TM) polarized wave on a planar metallic surface, the ratio of energy in the dielectric media to that in the metal can be calculated as  $\eta = P_d/P_m = (\text{Re}\{-\varepsilon_m \text{Re}\{k_y^m\}\})/(\text{Re}\{\varepsilon_d \text{Re}\{k_y^d\}\})$ . Figure 1 shows this ratio in terms of the wavelength, where we use the experimental parameters data for the metal.<sup>23</sup> It can be seen that, as the frequency decreases (below the surface plasmon frequency), the energy decays slower in the dielectric medium while faster in the metal, therefore, the ratio  $\eta$  increases with the wavelength of the SPPs. For silver at 1000 nm, the energy in the air can be more than  $10^3$  times that in the metal, and at 600 nm, this ratio is still larger than  $10^2$ . Since in frequencies below the surface plasmon frequency of the metal most of the SPP is traveling in the dielectric part of the waveguide, the use of transformation optics to redesign and optimize only the dielectric part of the waveguide is not a severe restriction and allows greatly improved functionality.

## RESULTS AND DISCUSSION

**Confining SPPs on a Non-uniform Metal Surface.** The roughness of a metallic surface can change the properties of the SPPs,<sup>24</sup> resulting in the scattering of the SPP modes and an inefficient transmission of light energy. We study how SPP scattering off an imperfection on the surface of a metallic waveguide can be reduced by covering it with a dielectric layer, the properties of which are designed with transformation optics. Important about this example is that we will see that the material requirements on the dielectric layer are not far-fetched. We start with the simplest case, where there is a triangular-shaped bump (or crevice) of silver on the silver/air interface, and we limit our discussions to a 2D scenario. By applying the following transformation<sup>25,26</sup>

$$\begin{aligned} x' &= x, \quad y' = \frac{H_2 - H_1}{H_2} y + \frac{D - x \text{sgn}(x)}{D} H_1, \\ z' &= z \end{aligned} \quad (1)$$

where  $(x, y, z)$  and  $(x', y', z')$  correspond to the coordinates of the initial virtual space and the transformed physical space, respectively. The large triangular region ABC in Figure 2 is mapped to the yellow polygonal region ABPC. Therefore, by engineering the materials in the yellow region (which we refer to as the surface plasmon wave adapter in all the following parts of the paper), it is possible to confine surface plasmon modes on the modulated surfaces and to guide the light energy around the imperfection bump with high efficiency.

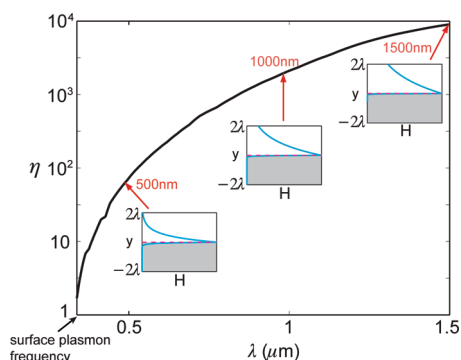


**Figure 1.** Ratio of energy in the dielectric media to that in the metal. The insets show the magnitude of the magnetic fields for working wavelengths of 500, 1000, and 1500 nm.

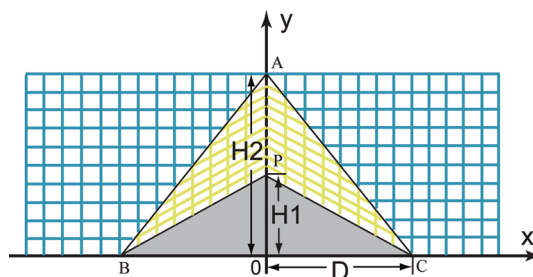


**Figure 2.** Coordinate transformation which compresses a triangular region along the  $y$  axis into the region denoted in yellow.

Considering TM polarization, the material parameters of the surface plasmon wave adapter are obtained as

$$\begin{aligned} \bar{\varepsilon} &= \varepsilon_b \begin{bmatrix} \frac{H_2}{H_2 - H_1} & -\text{sgn}(x) \frac{H_1 H_2}{(H_2 - H_1)D} \\ -\text{sgn}(x) \frac{H_1 H_2}{(H_2 - H_1)D} & \frac{H_2 - H_1}{H_2} + \frac{H_2}{H_2 - H_1} \left(\frac{H_1}{D}\right)^2 \end{bmatrix}, \\ \mu_{zz} &= \frac{H_2}{H_2 - H_1} \end{aligned} \quad (2)$$

Equation 2 shows that the parameters of the adapter are spatially invariant. In order to further simplify the parameters and make them realizable with natural materials at optical frequencies, we consider reduced electromagnetic parameters by letting  $\mu_{zz} = 1$  while keeping  $\mu_{zz}\bar{\varepsilon}$  unchanged:<sup>27</sup>

$$\begin{aligned} \bar{\varepsilon} &= \varepsilon_b \begin{bmatrix} \left(\frac{H_2}{H_2 - H_1}\right)^2 & -\text{sgn}(x) \left(\frac{H_2}{H_2 - H_1}\right)^2 \frac{H_1}{D} \\ -\text{sgn}(x) \left(\frac{H_2}{H_2 - H_1}\right)^2 \frac{H_1}{D} & 1 + \left(\frac{H_2}{H_2 - H_1}\right)^2 \left(\frac{H_1}{D}\right)^2 \end{bmatrix}, \\ \mu_{zz} &= 1 \end{aligned} \quad (3)$$

Due to the symmetry in  $\bar{\varepsilon}$ , the permittivity tensor can be diagonalized by rotating the coordinate system, and all of the parameter components are positive. Therefore, there is a possibility to realize this surface plasmon wave adapter with a homogeneous anisotropic naturally occurring material, as we shall see below.

The validity of the parameters characterized by eq 3 is numerically studied. Figure 3 shows the normalized power flows for the SPPs at 590 nm on different silver

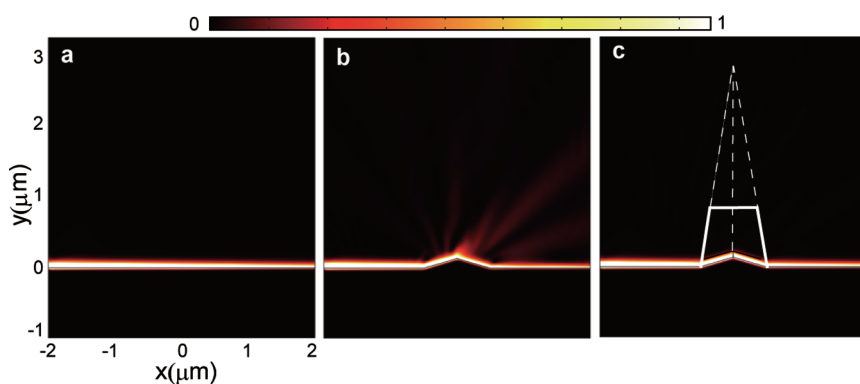


Figure 3. Normalized power flow of a TM polarized EM wave (at 590 nm) when SPPs propagate on (a) a smooth silver surface, (b) a protruded silver surface, (c) a protruded silver surface covered with the calomel crystal cladding.

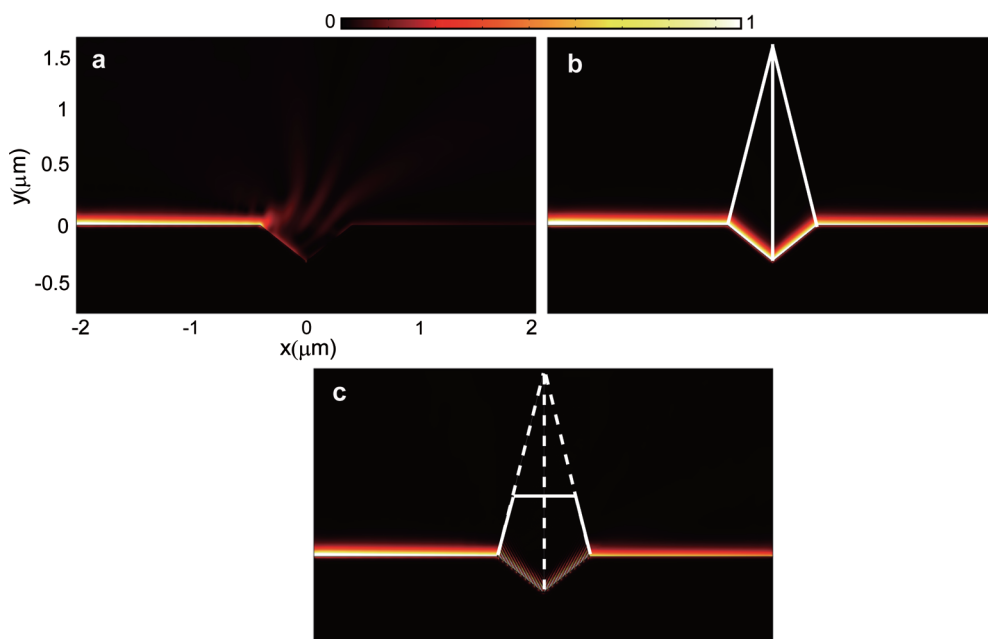


Figure 4. Normalized power flow of a TM polarized EM wave (at 632 nm) when SPPs propagate on (a) a silver surface with crevice, (b) a silver surface crevice covered by the transformational dielectric material, (c) a silver surface crevice covered by silicon grating structures.

surfaces where the permittivity of the background dielectric medium is  $\varepsilon_b = 5$ . Panel a depicts the SPP mode on a smooth surface, while panel b corresponds to a surface with a 144.4 nm high triangular bump, where pronounced scattering can be observed. After covering the bump with a cladding made of calomel (a mineral form) crystal, a naturally occurring material which is transparent at optical frequencies

$$\varepsilon = \begin{bmatrix} 3.893 & 0 \\ 0 & 7.054 \end{bmatrix}, \mu = 1$$

the SPPs are smoothly guided along the surface, as shown in panel c. Since most energy is confined near the surface of the metal, we can truncate the sharp tip of the cladding without affecting the function of the wave adapter, as indicated by the white solid line in panel c.

It is worth noticing that the anisotropy of a natural material is usually low and cannot be engineered as

desired. Although calomel crystal exhibits a relatively high value of birefringence (4 times higher than calcite, which has been recently used for an invisibility cloak in the visible spectrum<sup>28,29</sup>) as a naturally occurring crystal, it still can only work effectively for flat bumps and the adapter cannot be designed according to the shape of the bump. Grating-structured dielectric materials, which have effective anisotropic parameter profiles, provide a solution to this problem. According to the effective medium theory,<sup>30</sup> a composite medium comprising two different materials interlaced at the subwavelength scale can be approximated as a homogeneous medium with the anisotropic permittivity tensors expressed as  $\varepsilon_{\parallel} = r\varepsilon_1 + (1 - r)\varepsilon_2$  and  $\varepsilon_{\perp} = (\varepsilon_1\varepsilon_2)/(r\varepsilon_2 + (1 - r)\varepsilon_1)$ , where  $\varepsilon_1$  and  $\varepsilon_2$  are the permittivities of the two different materials and  $r$  denotes the filling factor of the constituent materials.

Figure 4a shows a sharp crevice on a silver surface (316 nm deep, 800 nm wide) which causes severe scattering of the SPP wave. An adapter is designed according to eq 3 to guide the SPP mode at 632 nm smoothly along the surface of the crevice (in this case,  $H_1$  is negative) where the resulting material parameters are

$$\varepsilon = \begin{bmatrix} 8.035 & 0 \\ 0 & 1.8755 \end{bmatrix}, \mu = 1$$

Panel b shows the effectiveness of the adapter made of this transformation medium. In practical applications, this anisotropic transformation medium can be realized by subwavelength silicon gratings, as shown in panel c. The pitch of the grating structure is 20 nm, which is

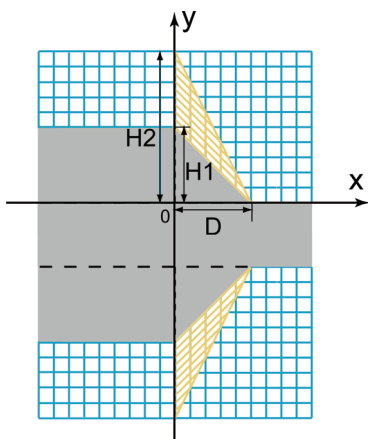


Figure 5. Coordinate transformation which compresses a trapezoidal region along the  $y$  axis into the region denoted in yellow.

much smaller than the wavelength in the background medium ( $\varepsilon_b = 4.67$ ), and the filling factor  $r = 0.5$ . Similarly, the top of the adapter can be truncated to save the material as well as the space.

**Adiabatic Mode Transformation between Metal Films with Short Taper.** A thin metal film can support SPPs, the energy of which largely extends into the dielectric medium. Consequently, this kind of SPP usually generates substantial scattering when propagating through a film of which the width is abruptly varied (as shown in Figure 5, where the gray region is the metal), leading to low transitioning efficiency. In plasmonic applications, tapers are always used to gradually couple SPP modes between waveguides of different widths.<sup>12,13</sup> However, there is a trade-off between adiabaticity and loss: a taper can be made very long and gradual so that the SPP is transformed very adiabatically, but then inherent loss of the metal will have eaten all SPPs at the taper end. Therefore, an optimum taper considering both loss and scattering is required. Here, we consider the case where SPPs propagate on an abruptly narrowed metallic film. The schematic of the transformation is depicted in Figure 5, and the finite-embedded transformation<sup>31</sup> applied here is similar to the one described by eq 1. As can be seen from the wave trajectories in Figure 5, the incoming waves from the right-hand side would be shifted in the  $y$  direction and abruptly be forced back on its old path at the boundary at  $x = 0$ . Consequently, the boundary is for simplicity not included in the calculation of the material properties for the SPP wave adapter. For the TM polarization, the simplified

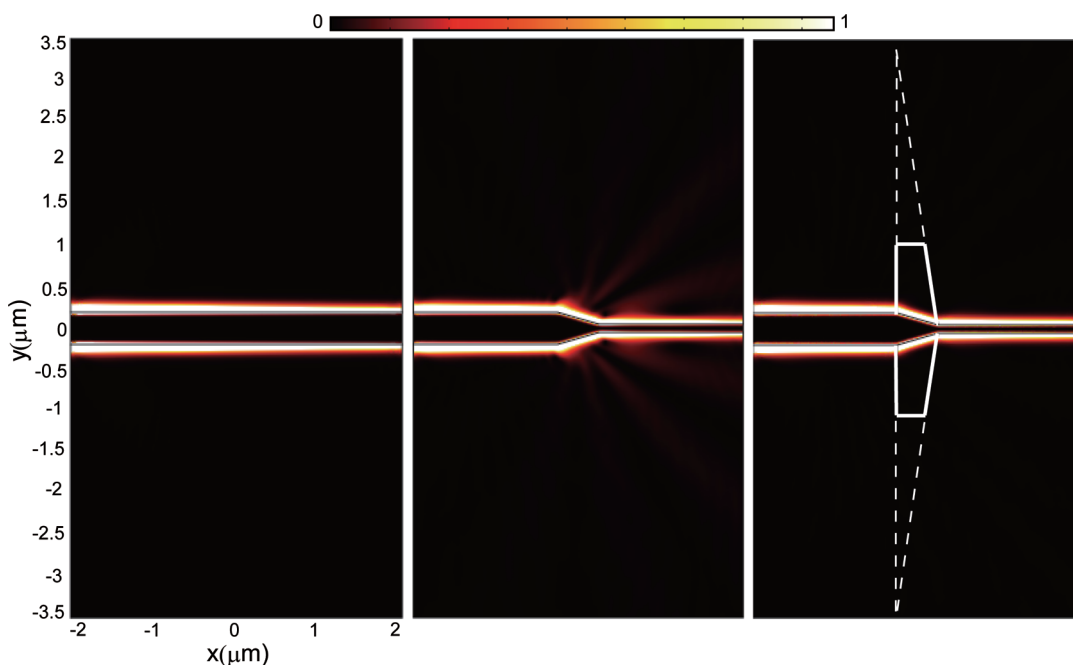
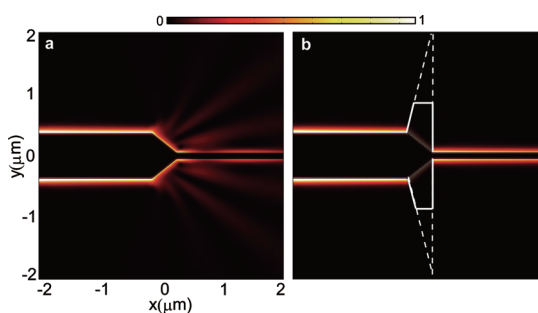


Figure 6. Normalized power flow of a TM polarized EM wave (at 590 nm) when SPPs propagate on the surface of (a) a 390 nm thick silver film, (b) a 390 nm thick silver film connected with a 100 nm thick silver film by a 500 nm long taper. (c) Tapered junction is covered by the calomel crystal.



**Figure 7.** Normalized power flow of a TM polarized EM wave (at 632 nm) when SPPs propagate on the surface of (a) a 732 nm thick silver film connected with a 100 nm thick silver film by a 400 nm long taper, (b) a 732 nm thick silver film connected with a 100 nm thick silver film. The tapered junction is covered by silicon grating structures.

electromagnetic parameters of the wave adapter are described as

$$\bar{\epsilon} = \epsilon_b \begin{bmatrix} \left(\frac{H_2}{H_2 - H_1}\right)^2 & -\left(\frac{H_2}{H_2 - H_1}\right)^2 \frac{H_1}{D} \\ -\left(\frac{H_2}{H_2 - H_1}\right)^2 \frac{H_1}{D} & 1 + \left(\frac{H_2}{H_2 - H_1}\right)^2 \left(\frac{H_1}{D}\right)^2 \end{bmatrix}, \quad (4)$$

$$\mu_{zz} = 1$$

To demonstrate the feasibility of this idea, we simulate two different cases, that is, one adapter made of a calomel crystal and one constructed with silicon gratings. In Figure 6, the SPP mode is excited on a silver film whose width is 390 nm. Figure 6b shows the 2D lateral view of a SPP propagating on the 390 nm wide film and scattered at the 500 nm long taper connected with a 100 nm wide silver film. By covering the conjunction with triangular claddings characterized by eq 4, as shown in Figure 6c, the SPP wave is shifted in the  $y$  direction and always confined at the silver/air surface when entering the claddings. The SPP modes are smoothly coupled to the narrow film, and the

scattering is significantly suppressed. As illustrated above, the adapter can be improved, and a relatively shorter taper can be achieved with silicon grating structures with the same settings as that in the previous section. Figure 7 corresponds to the case where the SPP modes are transferred from a 732 nm silver film to a 100 nm film by a 400 nm long taper, and similar beneficial effect of the adapter can be observed by using silicon gratings.

## CONCLUSION

Transformation optics can help to design clever claddings to confine the SPP waves on imperfect surfaces and to enhance the parameter regime of adiabatic mode transformation for surface plasmon polaritons in tapered nanowires toward much shorter tapers, thus reducing both loss and scattering of SPPs. With the holy grail in mind of transporting light from a single atom to a tiny metallic nanowire to finally an optical fiber with nearly unit efficiency, the wave adapter proposed here is a promising new optical component. Two different recipes are proposed to realize this adapter: the one using homogeneous anisotropic natural material and the other using subwavelength gratings.

Another potential application of this SPP adapter is in the rapid adiabatic nanofocusing of optical energy. The focusing effect of a tapered waveguide is associated with the vertex angle formed at the tip. Since large vertex angle at the tip corresponds to large radiative loss (or large scattering), a tapered waveguide with gradually varying cross section is usually used in nanofocusing. However, this means a longer propagation path of surface plasmons on the metal surface, resulting in more energy dissipation. The SPP adapter which enables a shorter taper offers a possible solution to this concern.

## METHODS

**Numerical Simulations.** The calculations are performed using the finite-element method (FEM) software package COMSOL Multiphysics. The material parameters of silver are taken from the experimental results,<sup>23</sup> and the imaginary part of the permittivity of silicon<sup>32</sup> is considered in the simulations to evaluate the effect of the material loss on the performance of the adapter.

**Energy Ratio of Dielectric to Metal.** For a TM polarized wave on a planar metallic surface, the tangential component of the magnetic field and normal component of the electric field in the dielectric medium are

$$H_z^d = H_0 e^{ik_x x - k_y^d y}, \quad E_y^d = \frac{k_x}{\omega \epsilon_d} H_0 e^{ik_x x - k_y^d y} \quad (5)$$

Likewise, the tangential component of the magnetic field and normal component of the electric field in the metal are

$$H_z^m = H_0 e^{ik_x x + k_y^m y}, \quad E_y^m = \frac{k_x}{\omega \epsilon_m} H_0 e^{ik_x x + k_y^m y} \quad (6)$$

where  $k_x = k_0((\epsilon_m \epsilon_d)/(\epsilon_m + \epsilon_d))^{1/2}$

$$k_y^d = \sqrt{k_x^2 - \epsilon_d k_0^2} = \frac{\epsilon_d k_0}{\sqrt{-\epsilon_m - \epsilon_d}}$$

$$k_y^m = \sqrt{k_x^2 - \epsilon_m k_0^2} = -\frac{\epsilon_m k_0}{\sqrt{-\epsilon_m - \epsilon_d}}$$

Here,  $\epsilon_m$  and  $\epsilon_d$  correspond to the permittivity of the metal and the dielectric medium, respectively. Therefore, the ratio of energy in the dielectric media to that in the metal can be obtained as

$$\eta = \frac{P_d}{P_m} = \frac{\frac{1}{2} \int dy \operatorname{Re}\{E_y^d \times H_z^{d*}\}}{\frac{1}{2} \int dy \operatorname{Re}\{E_y^m \times H_z^{m*}\}} = \frac{\operatorname{Re}\{-\epsilon_m \operatorname{Re}\{k_y^m\}\}}{\operatorname{Re}\{\epsilon_d \operatorname{Re}\{k_y^d\}\}} \approx \operatorname{Re}\left\{\frac{\epsilon_m^2}{\epsilon_d^2}\right\} \quad (7)$$

**Acknowledgment.** The work is supported by Hans Christian Ørsted postdoctoral fellowship as well as by the Danish Research Council for Technology and Production Sciences (FTP Grants 274-07-0080 and 274-07-0379).

## REFERENCES AND NOTES

- Gramotnev, D. K.; Bozhevolnyi, S. I. Plasmonics beyond the Diffraction Limit. *Nat. Photonics* **2010**, *4*, 83–91.
- Economou, E. N. Surface Plasmons in Thin Films. *Phys. Rev.* **1969**, *182*, 539–554.
- Sarid, D. Long-Range Surface-Plasma Waves on Very Thin Metal Films. *Phys. Rev. Lett.* **1981**, *47*, 1927.
- Takahara, J.; Yamagishi, S.; Taki, H.; Morimoto, A.; Kobayashi, T. Guiding of A One-Dimensional Optical Beam with Nanometer Diameter. *Opt. Lett.* **1997**, *22*, 475–477.
- Falk, A. L.; Koppens, F. H. L.; Yu, C. L.; Kang, K.; de Leon Snapp, N.; Akimov, A. V.; Jo, M.-H.; Lukin, M. D.; Park, H. Near-Field Electrical Detection of Optical Plasmons and Single-Plasmon Sources. *Nat. Phys.* **2009**, *5*, 475–479.
- Chang, D. E.; Sorensen, A. S.; Demler, E. A.; Lukin, M. D. A Single-Photon Transistor Using Nanoscale Surface Plasmons. *Nat. Phys.* **2007**, *3*, 807–812.
- Pile, D. F. P.; Gramotnev, D. K.; Oulton, R. F.; Zhang, X. On Long-Range Plasmonic Modes in Metallic Gaps. *Opt. Express* **2007**, *15*, 13669–13674.
- Nerkararyan, K. V. Superfocusing of a Surface Polariton in a Wedge-like Structure. *Phys. Lett. A* **1997**, *237*, 103–105.
- Oulton, R. F.; Pile, D. F. P.; Liu, Y. M.; Zhang, X. Scattering of Surface Plasmon Polaritons at Abrupt Surface Interfaces: Implications for Nanoscale Cavities. *Phys. Rev. B* **2007**, *76*, 035408.
- Elser, J.; Podolskiy, V. A. Scattering-Free Plasmonic Optics with Anisotropic Metamaterials. *Phys. Rev. Lett.* **2008**, *100*, 066402.
- Baumeier, B.; Leskova, T. A.; Maradudin, A. A. Cloaking from Surface Plasmon Polaritons by a Circular Array of Point Scatterers. *Phys. Rev. Lett.* **2009**, *103*, 246803.
- Verhagen, E.; Spasenovic, M.; Polman, A.; Kuipers, L. Nanowire Plasmon Excitation by Adiabatic Mode Transformation. *Phys. Rev. Lett.* **2009**, *102*, 203904.
- Tian, J.; Yu, S.; Yan, W.; Qiu, M. Broadband High-Efficiency Surface-Plasmon-Polariton Coupler with Silicon–Metal Interface. *Appl. Phys. Lett.* **2009**, *95*, 013504.
- Pendry, J.; Schurig, D.; Smith, D. Controlling Electromagnetic Fields. *Science* **2006**, *312*, 1780–1782.
- Leonhardt, U. Optical Conformal Mapping. *Science* **2006**, *312*, 1777–1780.
- Luo, Y.; Pendry, J. B.; Aubry, A. Surface Plasmons and Singularities. *Nano Lett.* **2010**, *10*, 4186–4191.
- Aubry, A.; Lei, D. Y.; Fernandez-Dominguez, A. I.; Sonnefraud, Y.; Maier, S. A.; Pendry, J. B. Plasmonic Light Harvesting Devices over the Whole Visible Spectrum. *Nano Lett.* **2010**, *10*, 2574.
- Luo, Y.; Aubry, A.; Pendry, J. B. Electromagnetic Contribution to Surface-Enhanced Raman Scattering from Rough Metal Surfaces: A Transformation Optics Approach. *Phys. Rev. B* **2011**, *83*, 155422.
- Lei, D.; Aubry, A.; Maier, S. A.; Pendry, J. B. Broadband Nanofocusing of Light Using Kissing Nanowires. *New J. Phys.* **2010**, *12*, 093030.
- Liu, Y.; Zentgraf, T.; Bartal, G.; Zhang, X. Transformational Plasmon Optics. *Nano Lett.* **2010**, *10*, 1991–1997.
- Huidobro, P. A.; Nesterov, M. L.; Martin-Moreno, L.; Garcia-Vidal, F. J. Transformation Optics for Plasmonics. *Nano Lett.* **2010**, *10*, 1985–1990.
- Kadic, M.; Guenneau, S.; Enoch, S. Transformational Plasmonics: Cloak, Concentrator, and Rotator for SPPs. *Opt. Express* **2010**, *18*, 12027–12032.
- Palik, E. D. *Handbook of Optical Constants of Solids*; Elsevier: New York, 1998.
- Raether, H. *Surface Plasmons: On Smooth and Rough Surfaces and on Gratings*; Springer: Berlin, 1988.
- Luo, Y.; Zhang, J.; Chen, H.; Ran, L.; Wu, B.-I.; Kong, J. A. Rigorous Analysis of Plane-Transformed Invisibility Cloaks. *IEEE Trans. Antennas Propag.* **2009**, *57*, 3926–3933.
- Zhang, J.; Luo, Y.; Mortensen, N. A. Transmission of Electromagnetic Waves through Sub-Wavelength Channels. *Opt. Express* **2010**, *18*, 3864–3870.
- Cummer, S. A.; Popa, B.-I.; Schurig, D.; Smith, D. R.; Pendry, J. B. Full-Wave Simulations of Electromagnetic Cloaking Structures. *Phys. Rev. E* **2006**, *74*, 036621.
- Chen, X.; Luo, Y.; Zhang, J.; Jiang, K.; Pendry, J. B.; Zhang, S. Macroscopic Invisibility Cloaking for Visible Light. *Nat. Commun.* **2011**, *2*, 176.
- Zhang, B.; Luo, Y.; Liu, X.; Barbastathis, G. Macroscopic Invisibility Cloak for Visible Light. *Phys. Rev. Lett.* **2011**, *106*, 033901.
- Rytov, S. M. Electromagnetic Properties of A Finely Stratified Medium. *Soviet Physics JETP* **1956**, *2*, 466–475.
- Rahm, M.; Cummer, S. A.; Schurig, D.; Pendry, J. B.; Smith, D. R. Optical Design of Reflectionless Complex Media by Finite Embedded Coordinate Transformations. *Phys. Rev. Lett.* **2008**, *100*, 063903.
- Bass, M.; DeCusatis, C.; Li, G.; Mahajan, V. N.; Stryland, E. V. *Handbook of Optics: Optical Properties of Materials, Non-linear Optics, Quantum Optics*; McGraw-Hill: New York, 2009.